Supporting Information

Residual Nanoscale Strain in Cesium Lead Bromide Perovskite Reduces Stability and Shifts Local Luminescence

Xueying Li[1], Yanqi Luo[2], Martin V. Holt[2], Zhonghou Cai[2] and David P. Fenning[1,2]

[1]Materials Science & Engineering Program, University of California, San Diego, La Jolla, CA 92093

[2]Department of Nanoengineering, University of California, San Diego, La Jolla, CA 92093

[3]Advanced Photon Source, Argonne National Laboratory, Argonne, IL 60439

COMSOL simulation

The Structural Mechanics module in COMSOL was used to simulate the induced strain from cooldown during crystallization of $CsPbBr_3$. In the 2D simulation, a 2-µm thick and 30-µm wide $CsPbBr_3$ crystal sits atop a quartz slide patterned with 100-nm Pt. The crystal is positioned its midline right above the edge of the Pt. A 0.5 µm fillet was included at the corners of the crystal and the Pt edge to reduce unrealistic edge effects in the simulation. The thermal parameters of Pt and quartz from the COMSOL built-in library were used. For $CsPbBr_3$, the thermal parameters from the study by Rakita et al.[1] were used. The $CsPbBr_3$ is considered to crystallize stress free at 100°C. The temperature of the crystal and the substrate is reduced to 20°C, and the $CsPbBr_3$ crystal is compressed at the substrate interface due to its large coefficient of expansion compared with the substrates. A lateral strain gradient in the $CsPbBr_3$ crystal forms from the Pt side to the quartz side induced by the difference in coefficients of thermal expansion of the substrate materials.

Electron Backscatter Diffraction

To identify the crystal phase, electron backscatter diffraction (EBSD) is measured on the crystal using an FEI Apero scanning electron microscopy and Oxford symmetry detector at 20 kV. The crystal structures of orthorhombic $CsPbBr_3$ ICSD # 97851, tetragonal $CsPbBr_3$ ICSD # 109295 and cubic $CsPbBr_3$ ICSD # 29073 were used to match the crystal phase.

Atomic Force Microscopy

The AFM image was obtained using a Veeco Scanning Probe Microscopy in tapping mode and scanning over a range of 50 µm by 70 µm at a resolution of 360 × 512 data points.

Benchtop X-ray diffraction

Powder XRD spectra were taken by a Bruker AXS D8 Discover diffractometer in parallel beam geometry with Cu Kα radiation (λ=1.5418 Å). The height alignment accessory was used for accurate strain calculation.

Materials	CTE (10^{-6} K^{-1})
$CsPbBr_3$[1]	37.7
Pt[2]	9.0
Quartz[3]	0.55
TiO_2[4]	2.57

Table S1. Coefficients of thermal expansion of $CsPbBr_3$, Pt, quartz and TiO_2

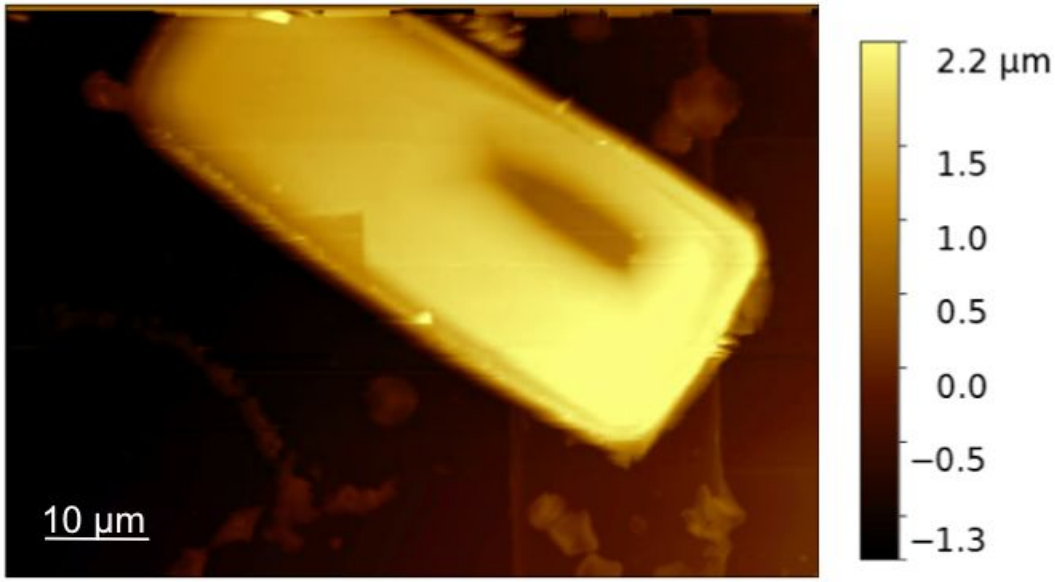

Figure S1. AFM of the $CsPbBr_3$ crystal measured by nanoXRD shows the crystal is 2-µm thick with a flat smooth surface except for one large void on the right of the crystal. The roughness Ra is around 40 nm on the crystal excluding the void.

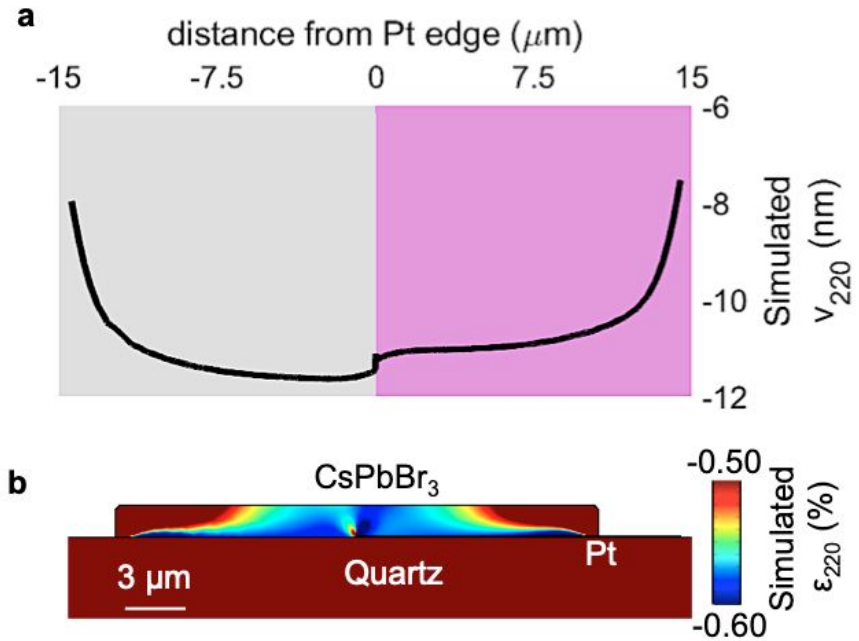

Figure S2. (a) Simulated displacement of a 2-um thick $CsPbBr_3$ crystal on Pt-patterned quartz substrate. (b) COMSOL mechanical simulation of the out-of-plane strain in a the $CsPbBr_3$ crystal on Quartz/Pt substrate.

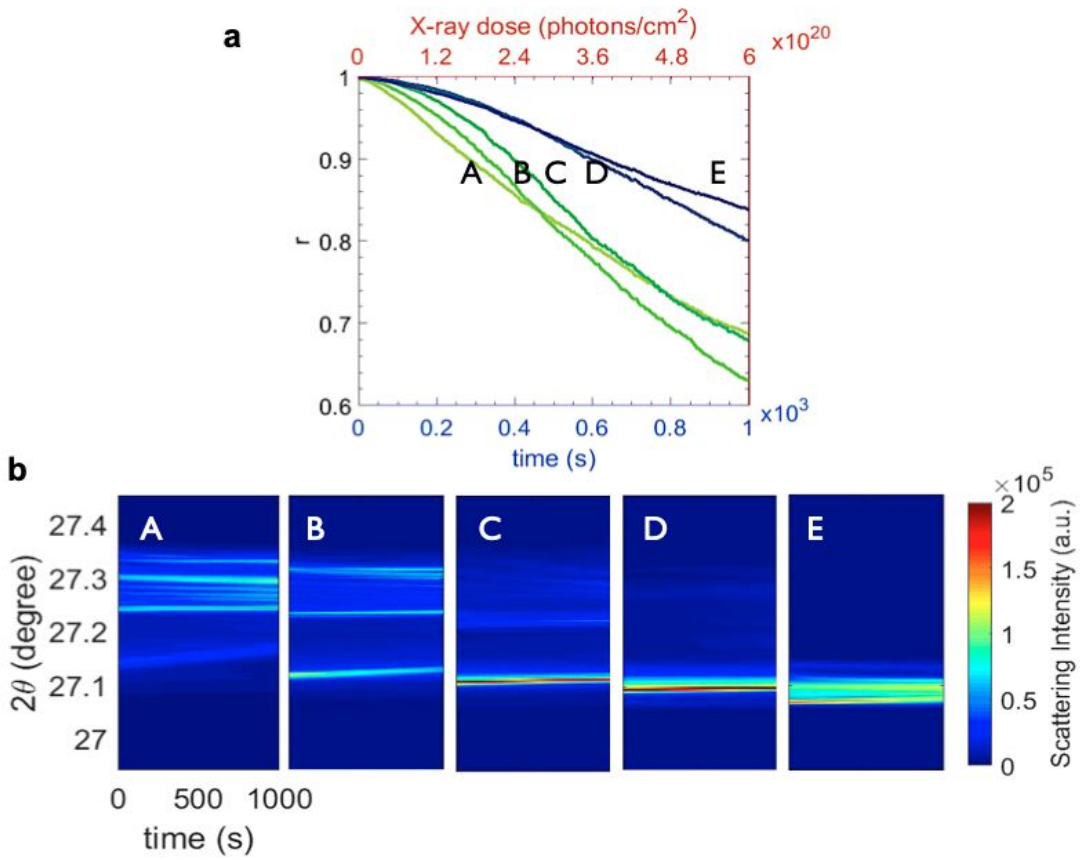

Figure S3. (a) Correlation Coefficient of diffraction images as a function of time under X-ray at five positions on the strained crystal indicated in Figure 2. (b) Waterfall plot of degrading diffraction patterns at positions A, B, C, D and E indicated in Figure 2.

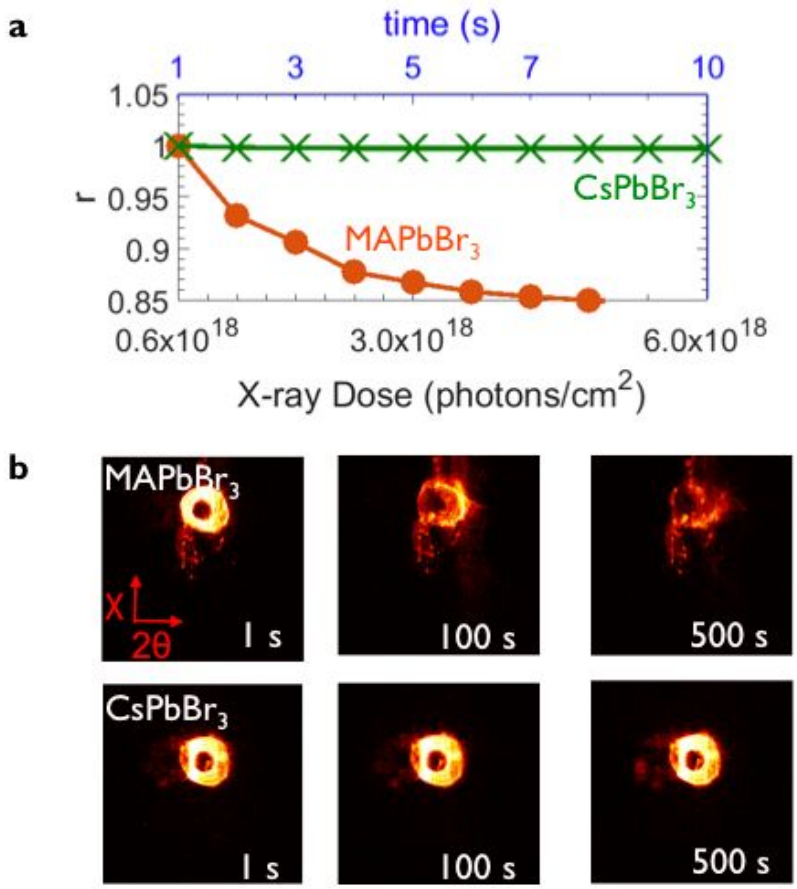

Figure S4. (a) Correlation coefficient r of the diffraction image vs. accumulated X-ray dose shows that $CsPbBr_3$ (green curve) are much more stable than $MAPbBr_3$ (red curve). (b) Diffraction images of $MAPbBr_3$ and $CsPbBr_3$ diffraction at 1, 100 500s showing the relatively stable $CsPbBr_3$ under X-ray irradiation and the loss of long range order in the hybrid perovskite.

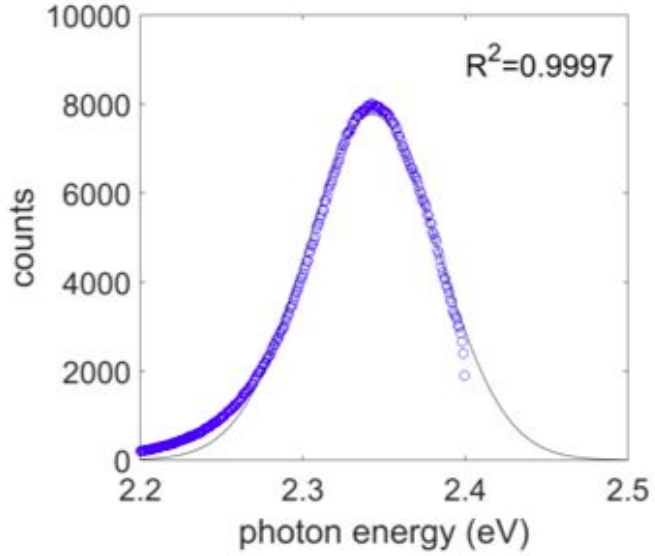

Figure S5. Example of single Gaussian fit of PL spectrum of $CsPbBr_3$ from μ-PL.

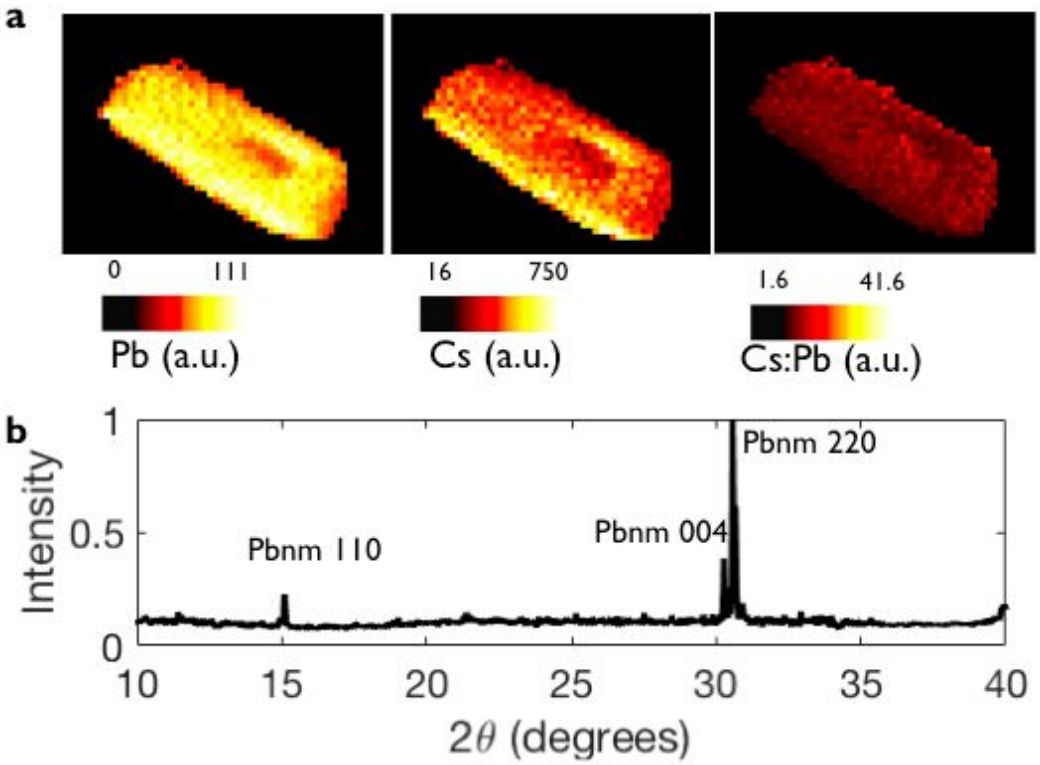

Figure S6. (a) Pb, Cs, Cs/Pb ratio maps in XRF. (b) Powder XRD of the $CsPbBr_3$ sample measured by nanoXRD.

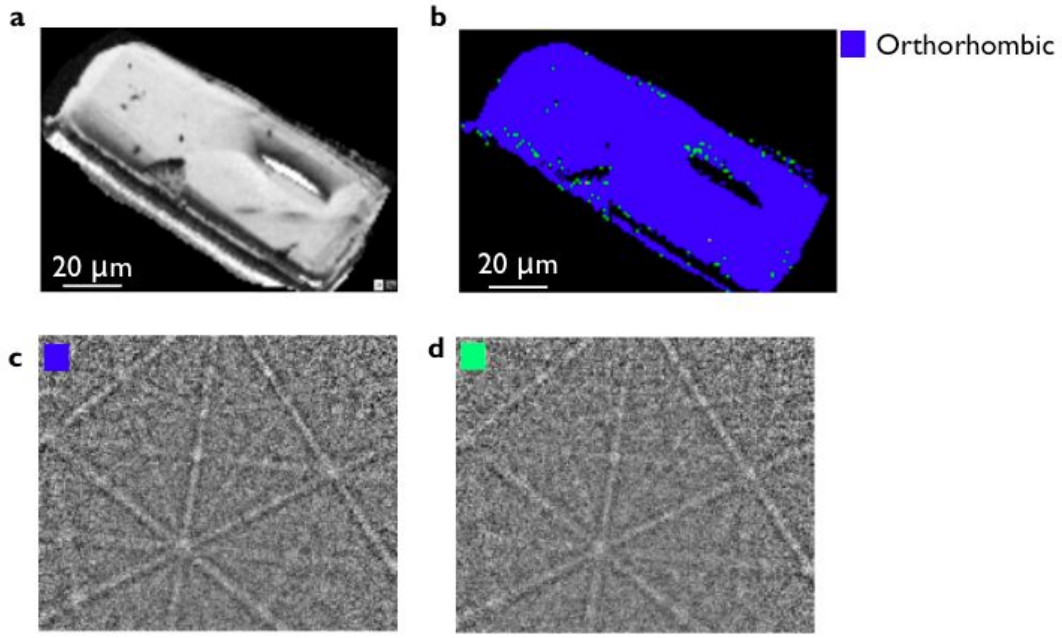

Figure S7. (a) SEM image of the $CsPbBr_3$ crystal measured after nanoXRD. (b) EBSD phase map of the $CsPbBr_3$ crystal shows the crystal is orthorhomic $CsPbBr_3$ with space group Pbnm. The green dots are not automatically identified as orthorhombic phase in the software, due to poorly indexed orthorhombic patterns, as shown by (c) the Kikuchi pattern of a blue point identified as orthorhombic $CsPbBr_3$ and (d) the Kikuchi pattern of a poorly-indexed (green) point identified mistakenly as cubic $CsPbBr_3$. The symmetry and pattern in (d) precisely matches that of (c).

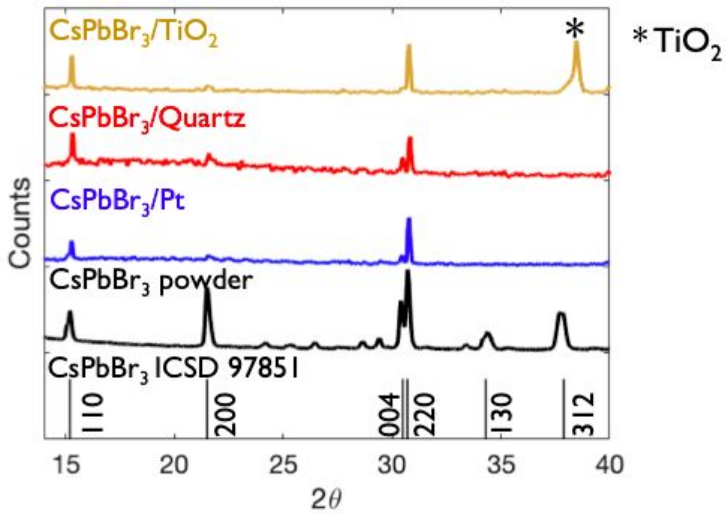

Figure S8. Powder XRD patterns of crystals on TiO2, Quartz, Pt, scraped powder from drop casted crystals on glass slides and major peaks of $CsPbBr_3$ in ICSD 97851.

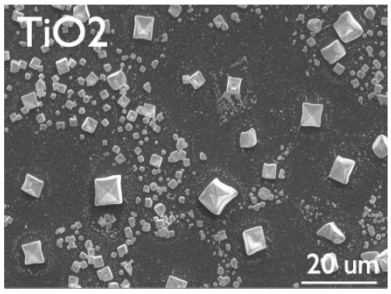

Figure S9. SEM image of $CsPbBr_3$ crystal stamped on TiO_2.

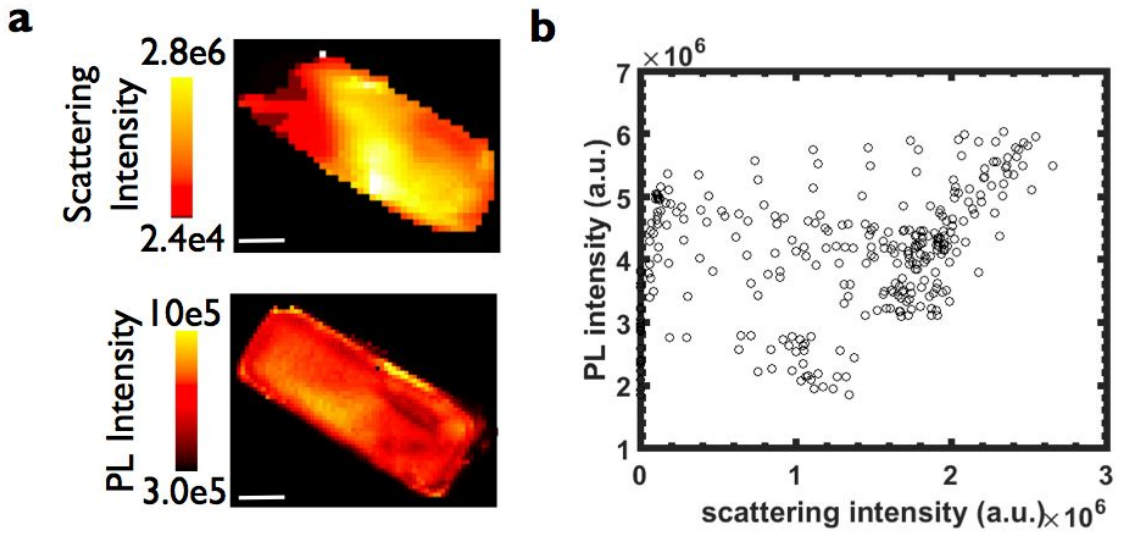

Figure S10. (a) Scattering intensity map from nanoXRD and PL intensity map from microPL on the same $CsPbBr_3$ crystal. (b) Scatter plot of PL intensity versus scattering intensity shows non-association. Scale bar is 10 μm in (a).

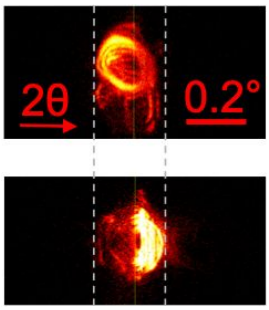

Figure S11. Diffraction patterns of two different spots on the mosaic $CsPbBr_3$ crystal in Figure 5. Gray lines are for eye guidance.

Supporting Information

References

(1) Rakita, Y.; Cohen, S. R.; Kedem, N. K.; Hodes, G.; Cahen, D. Mechanical Properties of APbX 3 (A = Cs or CH3NH3; X = I or Br) Perovskite Single Crystals. *MRS Commun.* **2015**, *5* (04), 623–629.

(2) Nix, F. C.; MacNair, D. The Thermal Expansion of Pure Metals. II: Molybdenum, Palladium, Silver, Tantalum, Tungsten, Platinum, and Lead. *Phys. Rev.* **1942**, *61* (1–2), 74–78.

(3) Jay, A. H. The Thermal Expansion of Quartz by X-Ray Measurements. *Proc. R. Soc. A Math. Phys. Eng. Sci.* **1933**, *142* (846), 237–247.

(4) Lee, C.-C.; Tien, C.-L.; Sheu, W.-S.; Jaing, C.-C. An Apparatus for the Measurement of Internal Stress and Thermal Expansion Coefficient of Metal Oxide Films. *Cit. Rev. Sci. Instruments* **2001**, *72*, 4189.